Acid-Catalyzed Rearrangements of 3-Aryloxirane-2-Carboxamides: Novel DFT Mechanistic Insights

Zheng-Wang Qu,*[a] Hui Zhu,[a] Sergey A. Katsyuba,[b] Vera L. Mamedova,[b] Vakhid A. Mamedov,*[b] and Stefan Grimme*[a]

Efficient synthesis of 3-arylquinolin-2(1*H*)-ones and *N*-(2-carboxyaryl)-oxalamides from protic acid-catalyzed rearrangements of 3-aryloxirane-2-carboxamides was achieved recently but not well understood. In contrast to the classical Meinwald rearrangement, extensive DFT calculations reveal that the proximal aryl and amide groups have strong synergetic effects to control the amide-aided and aryl-directed oxirane-opening and further rearrangement sequences. The *ortho*-nitro substituent of the proximal aryl is directly involved in a nucleophilic oxirane ring-opening, the amide C=O is an important proton shuttle for facile H-shifts, while the *N*-aryl may act as a potential ring-closing site via Friedel-Crafts alkylation. The mechanistic insights are useful for rational design of novel synthesis by changing the aryl and amide functional groups proximal to the oxirane ring.

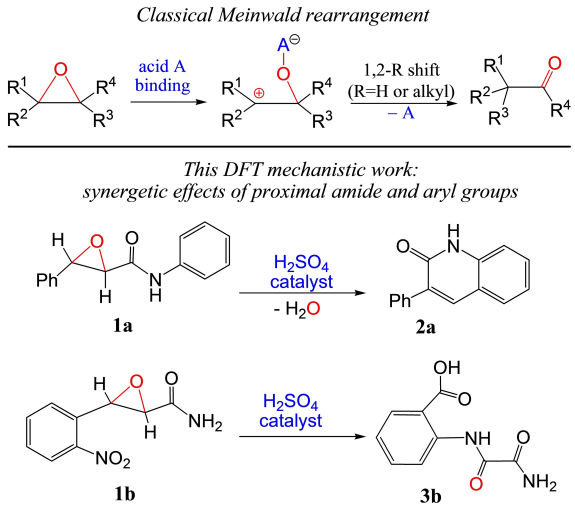

Scheme 1. Classical Meinwald rearrangement of monofunctional oxiranes (top) and acid-catalyzed rearrangements of 3-aryloxirane-2-amides **1 a** and **1 b** for the respective syntheses of 3-phenylquinolin-2(1*H*)-one **2 a** and *N*-(2-carboxyphenyl)-oxalamide **3 b**. Strong synergetic effects of the proximal amide and aryl functional groups are revealed by our extensive DFT calculations, which are useful for rational design of novel synthetic approaches.

Oxiranes (or epoxides) containing a saturated CCO three-membered ring are one of the most versatile classes of organic compounds available to the synthetic chemist which are frequently used in atom-economical rearrangement reactions.[1] In classical (Lewis or protic) acid catalyzed Meinwald rearrangements (Scheme 1),[2] mono-functional oxiranes are converted into neutral carbonyl compounds (aldehyde or ketone) via acid-induced C–O cleavage followed by 1,2-shift of a hydride or alkyl group within the resultant carbenium intermediate.[3] Recently, a series of intermolecular tandem Meinwald rearrangement reactions have also been developed.[4]

Alternatively, functional groups can be introduced as substituent to the oxirane ring to realize novel conversions via either synergetic or sequential rearrangements.[5] Recently, very interesting sulfuric acid (H_2SO_4) catalyzed rearrangements of 3-aryloxirane-2-amides in acetic acid (CH_3COOH) solution were achieved for very efficient one-pot synthesis of 3-arylquinolin-2(1*H*)-ones[5c] and *N*-(2-carboxyaryl)-oxalamides[5b] (Scheme 1), tentatively assumed to be initialized by the classical Meinwald rearrangement (forming neutral carbonyl intermediates), and followed by intramolecular electrophilic Friedel-Crafts alkylation of the amide *N*-aryl or nucleophilic addition to the nitro group.[5b,c] Quinolin-2-ones and oxalamides are omnipresent in naturally occurring and synthetic compounds displaying a broad range of pharmacological activities and practical applications.[6] It is still desirable to gain deep mechanistic insights into such novel synthetic approach, especially the role of the amide and 2-nitroaryl functional groups proximal to the central oxirane ring, which can be very helpful for further rational design of more efficient and novel synthesis of new compounds.

In this theoretical work, extensive DFT calculations at the PW6B95-D3+COSMO-RS //TPSS-D3+COSMO level in acetic acid solution (see below for computational details) are

[a] Dr. Z.-W. Qu, Dr. H. Zhu, Prof. S. Grimme
Mulliken Center for Theoretical Chemistry
University of Bonn
Beringstr. 4
53115 Bonn (Germany)
E-mail: qu@thch.uni-bonn.de
grimme@thch.uni-bonn.de
[b] Prof. S. A. Katsyuba, Dr. V. L. Mamedova, Prof. V. A. Mamedov
Arbuzov Institute of Organic and Physical Chemistry
FRC Kazan Scientific Center of RAS
Arbuzov Str. 8
420088 Kazan (Russia)
E-mail: mamedov@iopc.ru

Supporting information for this article is available on the WWW under https://doi.org/10.1002/open.202000110

performed to explore the potential free-energy paths for the protic H_2SO_4 catalyzed rearrangement reactions of two typical 3-aryloxirane-2-carboxamides, i.e., *trans*-*N*,3-diphenyloxirane-2-carboxamide (**1 a**) and *trans*-3-(2-nitrophenyl)oxirane-2-carboxamide (**1 b**), which selectively lead to quite different 3-phenylquinolin-2(1*H*)-one (**2 a**) and *N*-(2-carboxyphenyl)-oxalamide (**3 b**) products, respectively (Scheme 1). In contrast to the classical acid-catalyzed Meinwald rearrangement of mono-functional oxiranes leading to neutral carbonyl compound intermediates, our DFT calculations clearly show that the proximal amide and aryl functional groups do show strong synergetic effects that profoundly affect the complete protic acid-catalyzed rearrangement process.

Our DFT calculations show that in acetic acid solution, the neutral H-bonded complex and the separated ion pair of HSO_4^- and $CH_3C(OH)_2^+$ are 2.5 and 6.9 kcal/mol less stable than the solvated H_2SO_4 and CH_3COOH molecules, respectively, and thus are thermodynamically unfavourable. Moreover, the proton transfers from H_2SO_4 to the nitro, oxirane and amide oxygen sites of **1 b** are 19.0, 21.9 and 0.1 kcal/mol endergonic to form the corresponding protonated species along with the HSO_4^- anion. The selective and reversible protonation of **1 b** at the amide C=O site by H_2SO_4 is almost barrierless. Similarly, the selective protonation of **1 a** at the amide C=O site by H_2SO_4 is 1.1 kcal/mol endergonic over a rather low barrier of 2.7 kcal/mol, indicating a slightly reduced proton affinity of *N*-aryl substituted amide group. Moreover, our DFT calculations suggest that most ionic and neutral species should exist as monomeric rather than hydrogen-bonded complexes due to the high dissolving power of acetic acid as solvent, which makes our DFT mechanistic study in such polar and protic solvent simpler than expected.

The mechanism of H_2SO_4-catalyzed rearrangement of **1 a** is explored by our DFT calculations at first. As shown in Figure 1, the protonation of the amide C=O group of **1 a** by H_2SO_4 is only 1.1 kcal/mol endergonic to form the separated ions of $\mathbf{A}^+$ and HSO_4^- in solution. Due to the protonation-enhanced C=N double bond character, *trans*-to-*cis* conversion of the amide group in $\mathbf{A}^+$ is prevented by a high barrier of 29.7 kcal/mol to form $\mathbf{Ac}^+$ that is −0.8 kcal/mol more stable; for comparison, similar conversion within neutral **1 a** is 3.5 kcal/mol endergonic over a moderate barrier of 17.7 kcal/mol. Further proton transfer from the amide C=O to the oxirane oxygen within $\mathbf{A}^+$ may selectively cleave the phenyl-connected C–O bond, which is 8.1 kcal/mol endergonic over a rather low barrier of only 11.0 kcal/mol (via transition structure $\mathbf{TSB}^+$) to form the phenyl stabilized carbenium $\mathbf{B}^+$. The recently proposed[5c] cleavage of the C–O bond proximal to the electron-deficient amide group is prevented by a high barrier of 29.4 kcal/mol (via $\mathbf{TSA}^+$), and thus is kinetically less favourable. The regioselective oxirane ring-opening is thus strongly directed by the proximal π-electron-donating phenyl group,[3] aided by the proximal amide C=O group as proton shuttle. The subsequent *trans*-to-*cis* conversion of the amide group of $\mathbf{B}^+$ (via $\mathbf{TSC}^+$ over a low barrier of 12.4 kcal/mol) can bring the amide *N*-phenyl group more close to the benzylium-like cation center, facilitating the intramolecular Friedel-Crafts alkylation of the *N*-phenyl at the *ortho*-site possible (via $\mathbf{TSD}^+$) to form the arenium cation $\mathbf{D}^+$. Alternatively, the reactive $\mathbf{B}^+$ can be efficiently trapped by HSO_4^- to form the neutral complex **Bs**, followed by similar *trans*-to-*cis* conversion of the amide group (via **TSCs**) into **Cs** that may also lead to $\mathbf{C}^+$ after HSO_4^- elimination, which is kinetically more likely with an overall barrier of 21.9 kcal/mol and may avoid potential side reactions at reactive carbenium center. Subsequently, the new OH group of $\mathbf{D}^+$ may abstract the arenium proton from the same side of the C_5N-ring, which is −6.4 kcal/mol exergonic over a low barrier of 7.5 kcal/mol (via $\mathbf{TSE}^+$) to form the complex $\mathbf{E}^+$ with a bound water (H_2O)

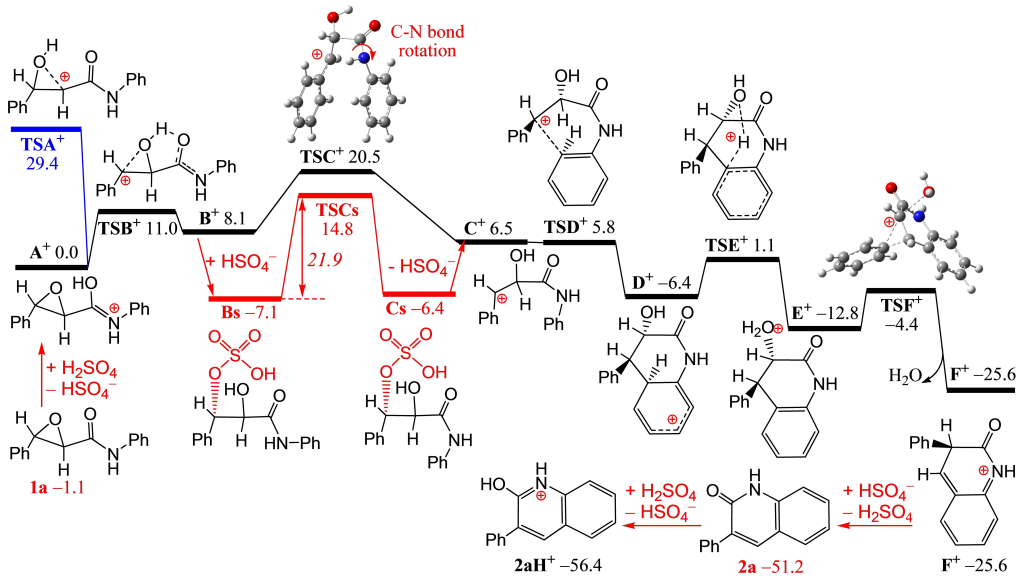

Figure 1. DFT computed free energy paths (in kcal/mol, at 298 K and 1 M concentration) for the H_2SO_4-catalyzed rearrangement of *trans*-*N*,3-diphenyloxirane-2-carboxamide (**1 a**) to 3-phenylquinolin-2(1*H*)-one (**2 a**). The free energies of neutral species (trapped or deprotonated by HSO_4^-) are shown in red. The H, C, N and O atoms in ball-stick models are shown as white, grey, blue and red balls. Partially breaking bonds are indicated by dashed lines.

molecule. The new H_2O molecule is then replaced by the adjacent phenyl group from the *opposite* ring side, which is −12.8 kcal/mol exergonic over a low barrier of 8.4 kcal/mol (via **TSF**$^+$) to form the site-3-carbon-protonated product **F**$^+$. The final proton transfer from **F**$^+$ to HSO_4^- is −25.7 kcal/mol exergonic and almost barrierless to form the neutral 3-phenyl-substituted **2a** that can be easily protonated by H_2SO_4 at the C=O oxygen site. The relative *trans*-configuration between the OH and Ph groups is crucial for the formation of 3-phenyl-substituted **2a**; 4-phenylquinolin-2(1*H*)-one is expected for the *cis*-configuration due to facile 1,2-H-shift instead. The strong synergetic effects of the proximal aryl and amide functional groups play a crucial role in directing the oxirane-ring opening as well as the facile intramolecular Friedel-Crafts alkylation. Such mechanism is quite different from the classical Meinwald rearrangement mechanism that involves a simple 1,2-shift of a hydride or alkyl group after oxirane opening to form carbonyl compounds.

As shown in Figure 2, the protonation of the amide C=O group of **1b** by H_2SO_4 is only 0.1 kcal/mol endergonic to form the separated ions of **G**$^+$ and HSO_4^- in solution. The *ortho*-nitro NO_2 substituent to the proximal phenyl actually leads to a different mechanism of oxirane-ring opening: the amide-to-oxirane proton transfer is now combined in a concerted way with the regioselective S_{N2} nucleophilic attack of one nitro oxygen toward the oxirane carbon connected to the phenyl, which is −6.9 kcal/mol exergonic over a low barrier of 17.6 kcal/mol (via transition structure **TSH**$^+$) to form the hetero-cyclic intermediate **H**$^+$ with a new C_3NO five-membered ring upon oxirane-ring opening. In contrast, similar nitro attack at the amide-connected oxirane carbon (via **TSHa**$^+$, see ESI) is prevented by a 11.1 kcal/mol higher barrier, while oxirane opening without nitro attack (via **TSG**$^+$) is kinetically 4.0 kcal/mol less favourable.

In the present case of the proximal 2-nitrophenyl group, the extra proton on the C_3NO ring of intermediate **H**$^+$ can be easily transferred to the adjacent amide C=O group (via **TSI**$^+$) over a low barrier of 18.6 kcal/mol, which in turn induces a more facile cleavage of the endocyclic N–O bond (via **TSJ**$^+$) and subsequent nitroso rotation (via **TSJc**$^+$) to form the low-lying intermediate **Jc**$^+$. In this way, one oxygen atom is transferred from the nitro group to oxidize the phenyl-connected oxirane carbon. Further nucleophilic attack of the nitroso oxygen aided by the protonation of the new C=O group enable the facile 1,3-shift of the cationic $CHOHCONH_2^+$ unit, which is −22.0 kcal/mol exergonic over a low free energy barrier of 10.9 kcal/mol (via **TSK**$^+$). The facile 1,2-H-shift along the C–N bond and concerted N–O bond cleavage (via **TSL**$^+$) eventually leads to the most stable form of the protonated product **L**$^+$, which is −55.5 kcal/mol exergonic over a barrier of 15.8 kcal/mol. The final deprotonation of **L**$^+$ by the anion HSO_4^- is −4.5 kcal/mol exergonic and almost barrierless to form the neutral product **3b** along with regenerated H_2SO_4 catalyst. Again, the aryl and amide functional groups proximal to the central oxirane ring lead to a new acid-catalyzed rearrangement mechanism.

Interestingly, when *trans*-3-(2-nitrophenyl)-*N*-phenyl-oxirane-2-carboxamide (**1c**) instead of **1b** was used as the substrate for which competitive rearrangements to both 3-(2-nitrophenyl) quinolin-2(1*H*)-one (**2c**) and *N*-(2-carboxyphenyl)-*N*-phenyl-oxalamide (**3c**) become possible, only the oxalamide product **3c** was formed exclusively.[5b] Fully consistent with such experimental results, the DFT-computed overall barriers for the catalytic rearrangements of very similar substrates **1a** and **1c** to the quinoline-2-one **2a** and the oxalamide **3b** are 21.9 and 18.6 kcal/mol, respectively, with the oxalamide product channel being kinetically 3 kcal/mol more favourable.

Our DFT mechanistic insights into the detailed role of various functional groups proximal to the central oxirane-ring are useful for further rational design of novel synthesis of

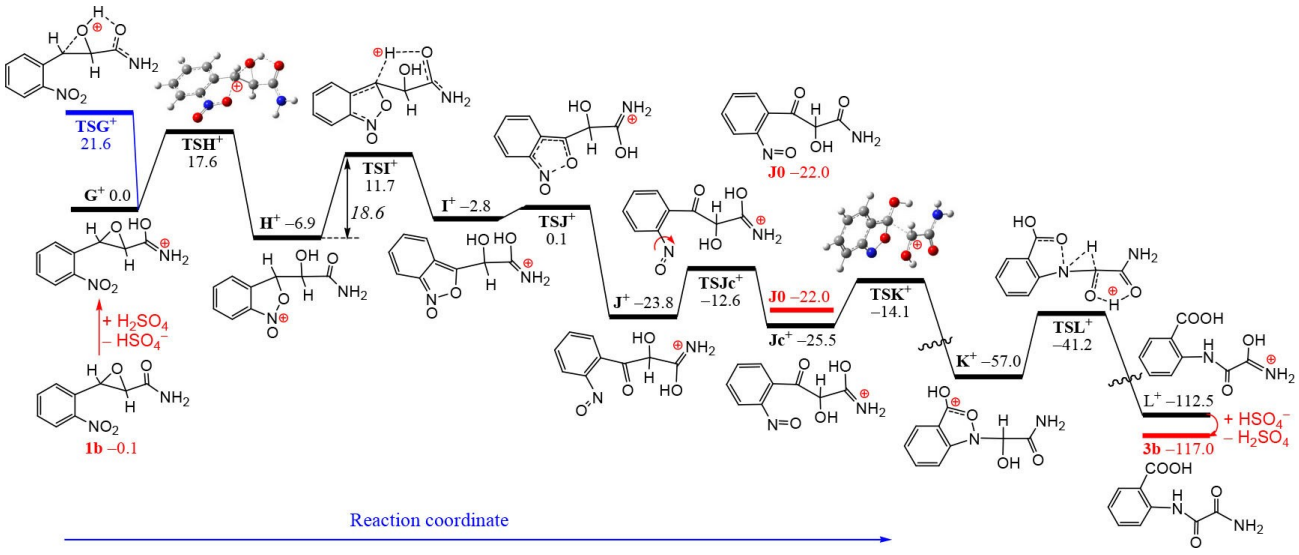

Figure 2. DFT computed free energy paths (in kcal/mol, at 298 K and 1 M concentration) for the H_2SO_4-catalyzed rearrangement of *trans*-3-(2-nitrophenyl) oxirane-2-carboxamide (**1b**). The free energies of neutral species after deprotonation by HSO_4^- are shown in red. The H, C, N and O atoms in ball-stick models are shown as white, grey, blue and red balls. Partially breaking bonds are indicated by dashed lines.

annulated compounds, for example, by replacing the *ortho*-NO_2 and amide NH_2 groups with other unsaturated functional groups such as NO, aryl and acyl groups. Such idea is further supported by our test DFT calculations showing that similar nucleophilic oxirane opening reactions can also be induced by simple NO, CHO and CH=CH_2 groups at the *ortho*-site of the proximal phenyl group (see ESI). Interestingly, it was experimentally known that the replacement of the amide NH_2 of **1b** with a phenyl group can lead to the same H_2SO_4-catalyzed rearrangement into 2-(2-oxo-2-phenylacetamido)benzoic acid,[5b] though an additional O_2-elimination channel to form 2-phenyl-3-hydroxyquinolin-4-one was also found very recently.[7]

In conclusion, detailed mechanisms of protic acid-catalyzed rearrangement reactions of multifunctional 3-aryloxirane-2-carboxamides for the synthesis of 3-arylquinolin-2(1*H*)-ones and *N*-(2-carboxyaryl)-oxalamides are revealed by state-of-the-art DFT calculations. In contrast to monofunctional Meinwald rearrangement, the amide and aryl functional groups proximal to the central oxirane ring lead to novel rearrangement sequences, with the amide C=O, amide *N*-aryl, aryl proximal to oxirane ring, and *ortho*-nitro functional groups acting as proton shuttle, potential Friedel-Crafts alkylation site, regioselective oxirane opening director, and nucleophile for S_{N2}-type oxirane opening, respectively. The mechanistic insights are useful for further rational design of novel synthesis by modifying the proximal functional groups.

Computational Methods

All DFT calculations are performed with the TURBOMOLE 7.3 suite of programs.[8] The structures are fully optimized at the TPSS-D3/def2-TZVP + COSMO (HCOOH) level, which combines the TPSS meta-GGA density functional[9] with the BJ-damped DFT–D3 dispersion correction[10] and the def2-TZVP basis set,[11] using the Conductor-like Screening Model (COSMO)[12] for acetic acid solvent (dielectric constant $\varepsilon = 6.19$ and diameter $R_{solv} = 2.83$ Å). The density-fitting RI–J approach[13] is used to accelerate the calculations. The optimized structures are characterized by frequency analysis (no imaginary frequency for true minima and only one imaginary frequency for transition states) to provide thermal free-energy corrections (at 298.15 K and 1 atm) according to the modified ideal gas-rigid rotor-harmonic oscillator model.[14]

More accurate solvation free energies in acetic acid are computed with the COSMO-RS model[15] (parameter file: BP_TZVP_C30_1601.ctd) using the COSMOtherm package[16] based on the TPSS-D3 optimized structures, corrected by +1.89 kcal/mol to account for the 1 mol/L reference concentration in solution. To check the effects of the chosen DFT functional on the reaction energies and barriers, single-point calculations at both TPSS-D3[9] and hybrid-meta-GGA PW6B95-D3[17] levels are performed using the larger def2-QZVP[11] basis set. Final reaction free energies (ΔG) are determined from the electronic single-point energies plus TPSS-D3 thermal corrections and COSMO-RS solvation free energies. As expected, the overall results from both DFT functionals are in good mutual agreement (0.2 ± 3.2 kcal/mol, mean difference between two functionals ± standard deviation) for reaction energies but somewhat higher reaction barriers (2.8 ± 3.6 kcal/mol) are found at the PW6B95-D3 level compared to the TPSS-D3 results. In our discussion, the more reliable PW6B95-D3 + COSMO-RS free energies (in kcal/mol, at 298.15 K and 1 mol/L concentration) are used unless specified otherwise. The applied DFT methods in combination with the large AO basis set provide usually accurate electronic energies leading to errors for chemical energies (including barriers) on the order of typically 1–2 kcal/mol. This has been tested thoroughly for the huge data base GMTKN55[18] which is the common standard in the field of DFT benchmarking.

Acknowledgements

The German Science Foundation (DFG) is gratefully acknowledged for financial support (Gottfried Wilhelm Leibnitz prize to S.G.).

Conflict of Interest

The authors declare no conflict of interest.

Keywords: DFT calculations · synergetic effects · oxirane opening · acid catalysis · reaction mechanism

[1] a) J. L. Jat, G. Kumar, *Adv. Synth. Catal.* **2019**, *361*, 4426–4441; b) K. Arata, K. Tanabe, *Catal. Rev. Sci. Eng.* **1983**, *25*, 365–420; c) A. S. Rao, S. K. Paknikar, J. G. Kirtane, *Tetrahedron* **1983**, *39*, 2323–2367.

[2] a) J. Meinwald, S. S. Labana, M. S. Chadha, *J. Am. Chem. Soc.* **1963**, *85*, 582–585; b) K. Maruoka, N. Murase, R. Bureau, T. Ooi, H. Yamamoto, *Tetrahedron* **1994**, *50*, 3663–3672; c) J. Prandi, J. L. Namy, G. Menoret, H. B. Kagan, *J. Organomet. Chem.* **1985**, *285*, 449–460.

[3] a) J. M. Fraile, J. A. Mayoral, L. Salvatella, *J. Org. Chem.* **2014**, *79*, 5993–5999; b) J. M. Coxon, R. Maclagan, A. Rauk, A. J. Thorpe, D. Whalen, *J. Am. Chem. Soc.* **1997**, *119*, 4712–4718; c) C. Zhou, J. Xu, *Prog. Chem.* **2011**, *23*, 174–189; d) X. Li, Z. Yang, J. Xu, *Curr. Org. Synth.* **2013**, *10*, 169–177; e) R. E. Parker, N. S. Isaacs, *Chem. Rev.* **1959**, *59*, 737–799.

[4] a) V. L. Mamedova, G. Z. Khikmatova, *Chem. Heterocycl. Compd.* **2017**, *53*, 976–978; b) M. R. Tiddens, R. J. M. Klein Gebbink, M. Otte, *Org. Lett.* **2016**, *18*, 3714–3717; c) C. C. Xu, J. X. Xu, *Org. Biomol. Chem.* **2020**, *18*, 127–134; d) C. C. Xu, Y. Lu, K. N. Xu, J. X. Xu, *Synthesis* **2020**, *52*, 602–608; e) Y. Shi, S. Li, Y. Lu, Z. Zhao, P. Li, J. Xu, *Chem. Commun.* **2020**, *56*, 2131–2134.

[5] a) S. Wang, C. Zhao, T. Liu, L. Yu, F. Yang, J. Tang, *Tetrahedron* **2016**, *72*, 7025–7031; b) V. A. Mamedov, V. L. Mamedova, G. Z. Khikmatova, E. V. Mironova, D. B. Krivolapov, O. B. Bazanova, D. V. Chachkov, S. A. Katsyuba, I. K. Rizvanov, S. K. Latypov, *RSC Adv.* **2016**, *6*, 27885–27895; c) V. A. Mamedov, V. L. Mamedova, S. F. Kadyrova, G. Z. Khikmatova, A. T. Gubaidullin, I. K. Rizvanov, S. K. Latypov, *Tetrahedron* **2015**, *71*, 2670–2679; d) V. A. Mamedov, V. L. Mamedova, S. F. Kadyrova, V. R. Galimullina, G. Z. Khikmatova, D. E. Korshin, A. T. Gubaidullin, D. B. Krivolapov, I. d. K. Rizvanov, O. B. Bazanova, O. G. Sinyashin, S. K. Latypov, *J. Org. Chem.* **2018**, *83*, 13132–13145; e) V. A. Mamedov, V. L. Mamedova, G. Z. Khikmatova, A. I. Samigullina, A. T. Gubaidullin, O. B. Bazanova, I. K. Rizvanov, O. G. Sinyashin, *Russ. Chem. Bull. Int. Ed.* **2015**, *64*, 2857–2864; f) H. Asahara, S. Matsui, Y. Masuda, N. Ikuma, T. Oshima, *Eur. J. Org. Chem.* **2012**, *2012*, 3916–3919; g) T. Oshima, H. Asahara, T. Koizumi, S. Miyamoto, *Chem. Commun.* **2008**, 1804–1806; h) H. Asahara, E. Kubo, K. Togaya, T. Koizumi, E. Mochizuki, T. Oshima, *Org. Lett.* **2007**, *9*, 3421–3424.

[6] a) C. B. M. Poulie, L. Bunch, *ChemMedChem* **2013**, *8*, 205–215; b) S. Heeb, M. P. Fletcher, S. R. Chhabra, S. P. Diggle, P. Williams, M. Cámara, *FEMS Microbiol. Rev.* **2011**, *35*, 247–274; c) F. Da Settimo, G. Primofiore, A. Da Settimo, C. La Motta, S. Taliani, F. Simorini, E. Novellino, G. Greco, A. Lavecchia, E. Boldrini, *J. Med. Chem.* **2001**, *44*, 4359–4369.

[7] V. A. Mamedov, V. L. Mamedova, A. T. Gubaidulin, D. B. Krivolapov, G. Z. Khikmatova, E. M. Mahrous, D. E. Korshin, O. G. Sinyashin, *Russ. Chem. Bull., Int. Ed.* **2020**, *69*, 510–516.

[8] a) TURBOMOLE V7.3, **2018**, development of University of Karlsruhe and Forschungszentrum Karlsruhe GmbH, 1989–2007, TURBOMOLE GmbH, since 2007; available from http://www.turbomole.com.

[9] J. Tao, J. P. Perdew, V. N. Staroverov, G. E. Scuseria, *Phys. Rev. Lett.* **2003**, *91*, 146401.
[10] a) S. Grimme, J. Antony, S. Ehrlich, H. Krieg, *J. Chem. Phys.* **2010**, *132*, 154104–154119; b) S. Grimme, S. Ehrlich, L. Goerigk, *J. Comput. Chem.* **2011**, *32*, 1456–1465.
[11] F. Weigend, R. Ahlrichs, *Phys. Chem. Chem. Phys.* **2005**, *7*, 3297–3305.
[12] A. Klamt, G. Schüürmann, *J. Chem. Soc. Perkin Trans. 2* **1993**, 799–805.
[13] a) F. Weigend, *Phys. Chem. Chem. Phys.* **2006**, *8*, 1057–1065; b) K. Eichkorn, F. Weigend, O. Treutler, R. Ahlrichs, *Theor. Chem. Acc.* **1997**, *97*, 119–124.
[14] S. Grimme, *Chem. Eur. J.* **2012**, *18*, 9955–9964.
[15] F. Eckert, A. Klamt, *AIChE J.* **2002**, *48*, 369–385.
[16] F. Eckert, A. Klamt, COSMOtherm, Version C3.0, Release 16.01; COSMOlogic GmbH & Co. KG, Leverkusen, Germany **2015**.
[17] Y. Zhao, D. G. Truhlar, *J. Phys. Chem. A* **2005**, *109*, 5656–5667.
[18] L. Goerigk, A. Hansen, C. Bauer, S. Ehrlich, A. Najibi, S. Grimme, *Phys. Chem. Chem. Phys.* **2017**, *19*, 32184–32215.

Manuscript received: April 21, 2020
Revised manuscript received: May 20, 2020